Advanced Powder Materials 2 (2023) 100114

Contents lists available at ScienceDirect

Advanced Powder Materials

journal homepage: www.keaipublishing.com/en/journals/advanced-powder-materials

Multiscale modelling of irradiation damage behavior in high entropy alloys

Fusheng Tan [a], Li Li [a], Jia Li [a,*], Bin Liu [b], Peter K. Liaw [c], Qihong Fang [a]

[a] State Key Laboratory of Advanced Design and Manufacturing for Vehicle Body, Hunan University, Changsha, 410082, China
[b] State Key Laboratory of Powder Metallurgy, Central South University, Changsha, 410083, China
[c] Department of Materials Science and Engineering, The University of Tennessee, Knoxville, TN, 37996, USA

ARTICLE INFO

Keywords:
High-entropy alloy
Multiscale modelling
Irradiation damage
Microstructure
Properties
Damage mechanism

ABSTRACT

The increasingly harsh environment of the nuclear reactors and the insurmountable flaws of in-service materials have created an urgent need for the development of the brand-new alloys. For last decade, the high-entropy alloys (HEAs), a novel composition-design strategy, have received much attention due to their promise for the nuclear fields. The application of the multiscale modelling is to explore the irradiation performance and underlying mechanisms of HEAs. Abundant results and data deepen the understanding of the irradiation response, and accelerate the development of advanced irradiation-resistant HEAs. This review introduces the state-of-art multiscale modelling used for studying the irradiated properties of HEAs. Representative irradiation-induced microstructures and properties, as well as damage, are summarized. By strengthening the application of multiscale modelling, a rational design of high irradiation-resistant HEAs is expected.

1. Introduction

The development of energy promotes the progress of human civilization, and the nuclear power has become an important part of the energy source of human society at present, and in the foreseeable future. However, several fatal flaws prevent the widespread application of the nuclear power, especially the limited safety and the lifespan of the nuclear-power plants (Fig. 1c). In-service Zr-based alloys for the nuclear fission reactors lack sufficient strength and corrosion resistance when the temperature rises to 600 °C [1]. For the most promising W-based alloys in the fusion-nuclear reactors, the low fracture toughness and small tritium retention restrict their operation temperature window and make them difficult to be prepared and processed [2]. The widely used oxide-dispersion-strengthening steels also suffer from their intrinsic low melting temperatures. Despite that the extensive efforts have been made to improve the irradiation resistance of in-service alloys, the development is still well below the demand of nuclear powers [3]. These challenges prompt the exploration of the brand-new alloy systems.

For last decade, the novel concepts of high entropy are introduced into the alloy design, triggering the birth of HEAs. Different with the traditional alloying strategy that adds small amounts of secondary elements to a principal element, the high-entropy alloys (HEAs) strategy involves the presence of multiple principal elements in high concentrations. Experiments show that HEAs have excellent mechanical, physical, and chemical properties [4–10]. Specifically, the potential of HEAs used for structural materials in nuclear power plants is proposed, attributing to the excellent combination of multiple key properties, such as high-temperature strength and stability, irradiation resistance, and corrosion resistance [11–13]. Representative HEAs are the well-studied face-centered-cubic (FCC) Cr–Mn–Fe–Co–Ni–Cu–Al systems consisting of transition metal elements [11], and the body-centered-cubic (BCC) Ti–Zr–Nb–Hf–Ta–W–V–Cr systems consisting of refractory elements [14]. To date, the research on the irradiation properties of HEAs is still on its early stage, and it has already demonstrated the excellent irradiation resistance [15–17]. It is expected that the irradiation resistance of HEAs can be further improved, particularly considering that a wide scope for the composition and microstructure design is still unexplored.

The rational material design should be based on the comprehensive understanding of underlying mechanisms, which is still missing for the high irradiation resistance of HEAs. The irradiation response of HEAs is controlled by multiscale mechanisms from the quantum to macroscopic scale [3]. Specifically, at the quantum scale, the electron structure affects the thermal conductivity during irradiation, and the energy of irradiation defect determines the thermodynamic stability. At the nanoscale, the atomic structure and energy of the irradiation clusters control the defect stability. At the microscopic scale, the interactions between irradiation defects and microstructures control irradiation damage. At the mesoscale, the evolution of dislocation networks contributes to the

* Corresponding author.
E-mail address: lijia123@hnu.edu.cn (J. Li).

https://doi.org/10.1016/j.apmate.2023.100114
Received 7 October 2022; Received in revised form 30 November 2022; Accepted 16 December 2022
Available online 13 February 2023

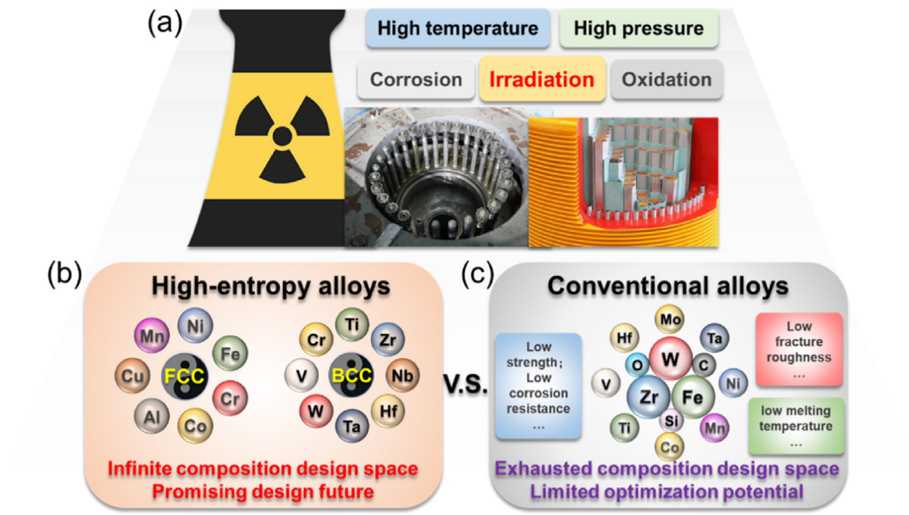

Fig. 1. Background of the structural materials for nuclear reactors. (a) Nuclear reactors and their harsh service conditions. Composition and advantage/flaw of the (b) HEA and (c) conventional structural material.

post-irradiation deformation. The coupling effects of multistage irradiation response at the cross multiple scales control irradiation lifespan.

At present, the ion irradiation combined with multiscale measurement and characterization is able to explore the irradiation response and underlying mechanism. However, the high cost and long cycles limit the wide application of experiment methods. Because of the development of computer science, multiscale modelling becomes effective and efficient computational material science tools to compensate experimental shortcomings. Several tools are widely utilized to study the irradiation response of alloys (Fig. 2) [2], including *ab initio* calculation for the quantum scale, molecular dynamics (MD) simulation for the nanoscale, discrete dislocation dynamics (DDD) for the mesoscale, and crystal plastic finite element method (CPFEM) for the macroscale. In addition, the cross-scale integrated computational method (ICM) is also applied. This review firstly introduces different computational methods and their applications on the irradiation behavior of HEAs (Section 2), then elaborates on the irradiation damage and mechanisms (Section 3.1), and summaries the irradiation-affected microstructures (Section 3.2) and properties (Section 3.3). The inclusions are the next (Section 4), followed by the prospects and future opportunities presented in the final part (Section 5).

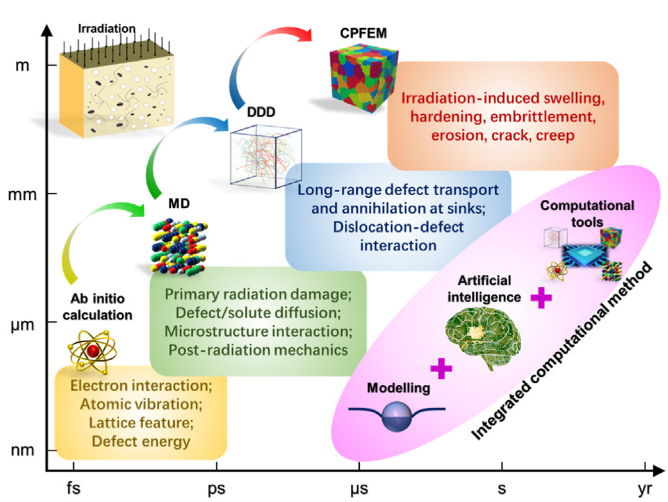

Fig. 2. Multiscale computational materials-science tools for irradiation studies. The limitations and applications of four computational tools (*ab initio* calculation, MD simulation, DDD, and CPFEM) and the ICM are summarized.

2. Advanced computational tools

2.1. Quantum scale: ab initio calculation

The *ab initio* calculation can obtain the ground-state properties of materials via describing electronic motion based on the density functional theory. At present, the *ab initio* calculation has the highest calculation accuracy among all theories and simulation methods. The greatest advantage of *ab initio* calculation is that it does not depend on any empirical parameters, only some basic physical constants (such as light speed and electron charge) are required. However, since the complicate electronic interaction is concerned, the calculation efficiency is extremely low. Only small calculation models (atomic number <200) and simple structures can be calculated, such as monocrystals and the crystals with simple defects (few point defects, dislocations, interfaces, and surfaces). To construct HEA models, the special quasi-random structures (SQS) method is most widely used, which optimizes the traditional supercell (SC) method by introducing correlation functions and applying Monte Carlo (MC) and genetic algorithms [18–21]. Other modelling methods, such as the virtual lattice approximation (VAC) and correlation potential approximation (CPA) techniques, are also available. The core electron-ion interactions are generally described by the Perdew-Burke-Ernzerhof (PBE) exchange-correlation energy functional within the generalized gradient approximation (GGA) [21].

Using *ab initio* calculation, the irradiation resistance of HEA can be evaluated by calculating the ground-state energy and electronic/atomic structure of the lattice and defect [23–25]. For example, the averaged partial density of states (PDOS) of *d* orbitals for elements in VTaCrW lattice are calculated, and the results show that 3d Cr and V exhibit a large DOS value at the Fermi energy, indicating that Cr and V atoms may present large displacement during irradiation [24]. Comparing the *d*-band smearing at the Fermi energy for Ni, NiCo, NiFe and NiCoFeCr HEAs, the highest-entropy NiCoFeCr alloy has much larger overall smearing. That means a short electron mean free path for HEA, which subsequently leads to a slow energy dissipation and enhances defect recombination in the vicinity of the collision cascades [26]. The formation and migration energies of the point defect (vacancy and interstitial) are key parameters that control the irradiation damage. By calculating the formation energies of stable interstitial dumbbells in VTaCrW HEA, it is found that the V–V, V–Cr, and Cr–Cr interstitial dumbbells have the lowest formation energies [24]. That leads to the enrichment of V and Cr around irradiation induced defects in W-based HEAs [25]. The distributions of migration energies of vacancy and interstitial in NiCoCr, NiCoFeCr [22] and VTaCrW [24] are studied, and a remarkable overlay region are observed (Fig. 3). That suggest an enhanced interaction between vacancies and interstitials in HEAs, which boosts defect recombination thus decreases irradiation damage. Since the BCC HEA exhibit larger overlay region between the distribution of migration energies compared with FCC HEAs, higher defect recombination rate is expected.

2.2. Nanoscale: MD simulation

The MD simulation is recognized as an effective method to reproduce the dynamic response of materials under mechanical, physical, and chemical conditions at the nanoscale. By simulating the atomic systems with limited atomic number (less than a few million), the microstructure evolution and nanoscale properties can be predicted. The atomic motion is controlled by the Newton laws [27]. The overall responses are obtained by analyzing the atomic trajectory and thermodynamic quantities based on statistical physics. The development of interatomic potential determines the acceptance of the MD method in material science. For HEAs, the potentials based on the embedded atom method (EAM) are most accepted [28,29], which simultaneously ensure precision and efficiency. Except that, the modified EAM (MEAM) potential is always used [30,31], which possesses higher precision but much lower efficiency because it considers the extra atomic binding angle. In addition, the Morse potential [32] and Lennard-Jones pair-potential [33] are also available. To simulate the collision cascades, the Ziegler-Biersack-Littmark (ZBL) potential is required, since the accurate atomic interaction is necessary when the atoms are extremely close to each other.

Based on MD simulation, nanoscale dynamic responses during and after irradiation can be obtained, including the collision cascades at the early state (<0.1ns) of irradiation damage (Fig. 4(a–c)), the thermodynamics or mechanics induced microstructure evolution at post-irradiation stages [34–36]. For instance, the simulation of the primary damage in NiCoCrFe HEA is conduct using MD simulation [34]. Fewer Frenkel Pairs and smaller defect cluster size of HEA are observed, which confirms the enhanced radiation resistance of HEAs (Fig. 4(d and e)). By analyzing the temperature evolution at the core of cascades and defect energies, the underlying mechanisms behind improved irradiation resistance are attributed to the low thermal conductivity and small binding energies of interstitial loops in HEA. The mechanism of radiation damage reduction in Ni, NiFe and NiCoCr alloys are investigated using MD method, with focus on the structure and motion of dislocations [36]. It is believed that the reduced dislocation mobility in HEAs suppresses the damage accumulation, thus leads to slower growth of large dislocation structures. By calculating the intensity and distribution of defect energies around grain-boundaries (GBs) in CuNiCoFe HEA, it is found that the local elemental ordering in GB greatly reduces the formation energies of interstitial [37]. That provides alternative explanation for the irradiation-induced segregation and enhanced radiation resistance for HEAs. These studies show that MD simulations are effective method to uncover the nanoscale mechanism of irradiation response in HEAs.

2.3. Mesoscale: DDD simulation

The DDD method is used to investigate the plasticity of irradiated materials at the mesoscale. By simulating the motion of dislocations in a finite space with adjustable stress fields, the dynamic interaction process between dislocations and irradiation defects in different alloys can be reproduced. The dislocation structure, motion, and reaction are constructed, based on classic dislocation theories and lower-scale simulations (*ab initio* calculation or MD) (Fig. 5a). Current DDD methods are limited to metals and dilute alloys. Further application on HEA requires the accurate stress field that considers the natural lattice-distortion feature of HEAs (Fig. 5b). This technical challenge is broken only recently. An advanced DDD framework for HEAs is created by introducing the heterogenous strain field that derives from nanoscale characterizations [38]. The deformation modes of the FeCoCrNiMn HEA obtained by DDD fit well with micropillar compression tests, confirming the validity of the novel DDD framework. Referring to the existing DDD

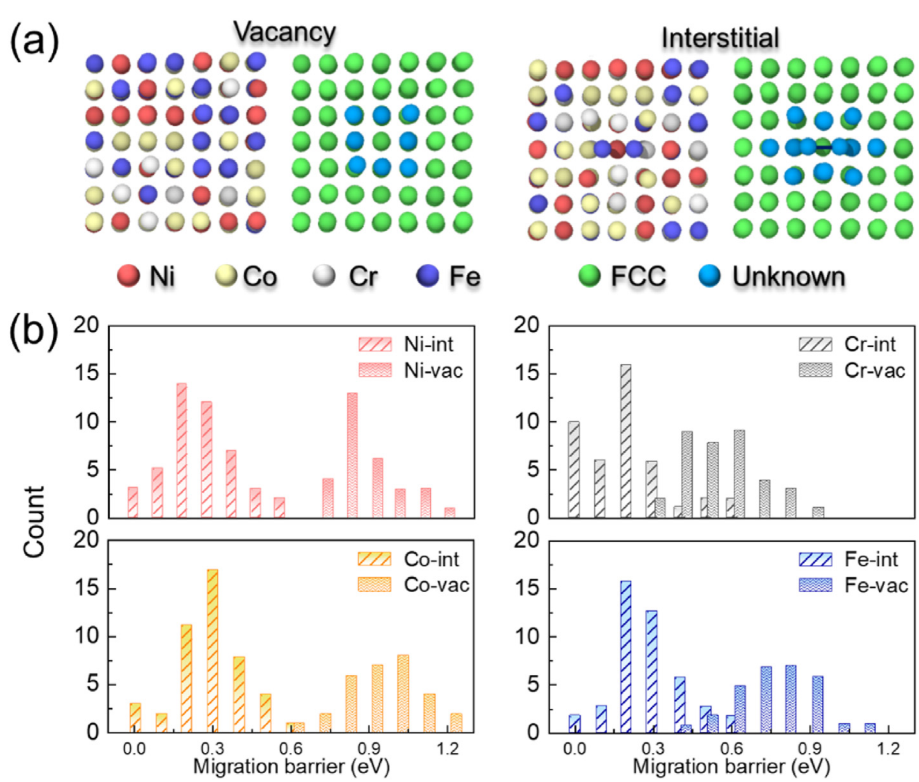

Fig. 3. *Ab initio* calculation for irradiation defect energies in HEAs. (a) Atomic models of vacancy and interstitial in HEAs. (b) Distributions of migration energies of vacancy and interstitial in NiCoFeCr HEA [22].

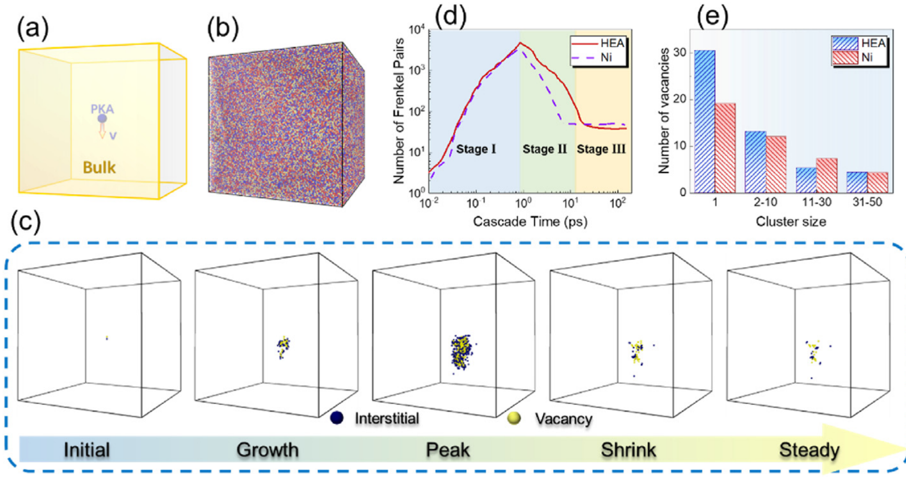

Fig. 4. MD simulations for dynamic process of cascades collision in HEAs. (a) The Schematic of cascades collision simulation, (b) the representative HEA model, (c) the typical evolution of point defects, (d) the evolution of Frenkel pairs, (e) as well as the atomic number of irradiation-induced point defects clusters are presented [34].

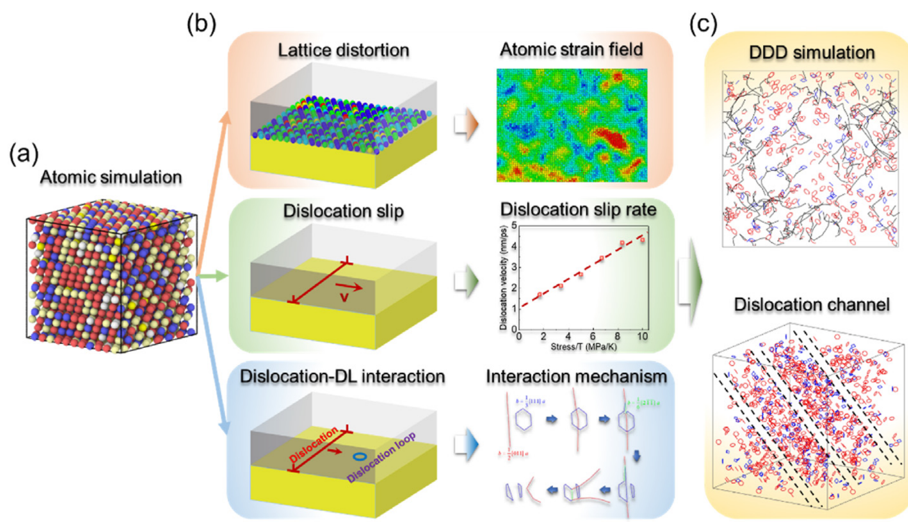

Fig. 5. Lattice-distortion-dependent DDD simulations for the plasticity of irradiated HEAs. (a) Atomic models used for simulate the (b) atomic lattice distortion, dislocation slip, and dislocation-DL interaction [38,39,42]. (c) DDD model that contains dislocations and DLs, and the deformation-induced dislocation channels observed in irradiated materials.

studies, the dislocation-based plastic origins of irradiated HEAs can be investigated by constructing the models containing irradiation-induced defects [39–41].

Based on DDD simulations, the irradiation hardening, brittleness, and their underlying mechanisms are investigated by constructing the models containing irradiation-induced DLs, SFTs, and voids (Fig. 5a) [39]. For example, by incorporating dislocation lines, DLs and SFTs in DDD models and determining their structure characteristics, the mesoscale plastic deformation of the irradiated Cu and Fe pillars is simulated. The structure, morphology and distribution of dislocations and defects, as well as the stress-strain relationship, are obtained. These results reveal the relationship between irradiation dose, loading mode and the magnitudes of strain bursts [40]. To uncover the size-dependent plastic flow localization in irradiated materials at the submicron scale, 3D DDD simulations with different sample sizes are performed. By analyzing the dislocation channel formation modes and irradiation defect density, it is found that the irradiation embrittlement mechanism transits from the irradiation-controlled to an intrinsic dislocation source controlled [41]. Because the structure and motion of dislocations and radiated defects, as well as their interactions, are strongly affected by the non-uniform stress field in HEAs [38], novel phenomenon and mechanisms at mesoscale are still mysteries, and need the urgent research.

2.4. Macroscale: CPFEM

The CPFEM combines the crystal plasticity theory and finite-element method, and serves as a bridge to connect the mechanical behaviors at mesoscopic and macroscopic scales. The success of CPFEM derives from a distinct advantage in describing the macroscale deformation based on microstructural evolutions. Multiple microscale plastic-deformation mechanisms are considered, including the dislocation activation, twining, phase transformation, and GB movement [43]. By assembling multiple grains with adjustable geometrical (such as shape, size, and orientation) and physical (such as elasticity and slip system) characteristics, the CPFEM captures the mechanical response of polycrystalline materials [43]. In CPFEM, the microstructure evolution is controlled by presetting theoretical models, which are established and simplified based on the data from experiments and lower-scale simulations (*ab initio* calculation, MD, and DDD) (Fig. 6). This approach ensures a high computational efficiency to approximate the macroscale experimental

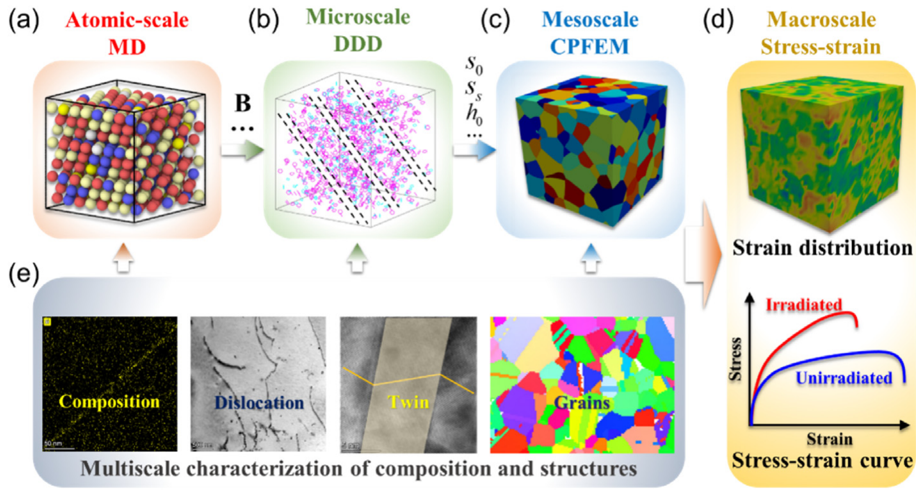

Fig. 6. Hierarchical multiscale CPFEM for the crystal plasticity of irradiated HEAs [42]. Based on (e) the multiscale characterization of composition and structures, the (a–c) multiscale simulations with bottom-up transfer of physical parameters are conducted. (d) The macroscale mechanical responses of irradiated HEAs.

results. To investigate the crystal plasticity of irradiated alloys using CPFEM, the key step is introducing the microscale mechanisms of plastic flow localization induced by irradiations. Note that the plastic flow localization is triggered by the formation of dislocation channel, which is further attributed to the annihilation/sweeping of irradiation-induced defects due to the continuous glide dislocations. Accordingly, some physically-based and phenomenological constitutive models are established [44–47]. For example, a crystal plasticity framework of irradiated BCC alloys accounting the irradiation-induced defects (primarily interstitial loops) is developed, in which the interaction between the glide dislocation and defect is described by the physical-mechanisms-driven constitutive model [45]. In addition, several crystal plasticity models for irradiated FCC alloys are also proposed [46,47], which account for the dislocation channeling controlled by the interactions between dislocations with interstitial loops and SFTs. Based on these frameworks, the effects of microstructure (grain size and orientation), mesoscopic factors (defects density and distribution), and thermo-mechanical conditions (temperatures and loading) on dislocation channeling and flow localization are studied.

Tremendous CPFEM have been conducted to investigate the mechanical behaviors of materials, with a few studies considering the effects of irradiation and features of HEAs. As representative, a mechanism-based crystal plasticity constitutive model for the Fe–Mn–Co–Cr–C HEA is developed, based on the experimental relationship between macroscopic ratcheting and microscopic mechanisms [43]. Using the CPFEM, the dynamic evolution of martensitic phase transformation and twinning is obtained, revealing the relationship among the microstructure evolution, deformation mechanism and mechanical response in HEAs. So far, CPFEM applied on the irradiation response of HEAs has not been available. Groundbreaking works can be realized through introducing the lattice-distortion effects of HEAs into irradiation models of traditional alloys [46]. Recently, a hierarchical multiscale crystal plasticity framework for plasticity of HEAs is proposed [42], which can capture the effect of the nano-micron-*meso*-scale structure on the mechanical properties. The framework unions the parameters of elasticity and dislocation-based plasticity from MD and DDD simulations. Especially, the core lattice distortion characteristic of HEAs is considered by introducing the lattice distortion strain field into the DDD models, to generate the plasticity-related parameters for CPFEM. Through introducing the mentioned irradiation-induced plasticity localization mechanisms into the hierarchical multiscale crystal plasticity framework (Fig. 6), the mesoscale crystal plasticity of irradiated HEAs can be expected.

2.5. Cross-scale: ICM

ICM is established by combining the computational tools (multiscale calculation), analytical tools (theoretical model), and artificial intelligence-assisted data analysis tools (machine learning) [48–51]. In this method, (i) multiscale calculation is used to obtain the raw dataset, generally including the compositions, structures, and properties; (ii) theoretical models are adopted to provide initial guidance; (iii) machine learning is served as the predictor of the target features. The predicted results are entered into the dataset for the next optimization, thus keeps getting closer to the target properties. Based on this technique, the material and product development cycle can be significantly reduced. For example, multi-disciplinary optimization is achieved by combining the calculation and analysis tools for the structural, flow and heat transfer into the design and manufacture of engine components. In this way, cumbersome tests of engine and related components are greatly simplified, which shorten the development cycle of engines by 2–6 years.

To date, ICM is applied to study the irradiation performance of materials, including the irradiation defect and property [52]. For example, the relationship between vacancy migration energies and local atomic environments in Fe-based alloys is mapped using the artificial-neural-networks machine learning model [53,54]. The large database (contains 30,000–100000 data) is generated within carefully designed local atomic environments through the nudged elastic band method using an empirical interatomic potential. Based on this, the accuracy and generalization ability of ICM are greatly expanded. The accuracy of machine learning model is further improved by using the defect database from *ab initio* calculations [55,56]. Recently, the support-vector-regression machine learning is applied to predict the vacancy formation and migration energies in NiFeCrCoCu HEA [57]. The energetic database is calculated based on the empirical interatomic potential. It is found that the accuracy can be achieved with a reduced training dataset, which only hundreds of calculations are needed. But the complicate chemical environment in HEAs is not included, because of the vast configurational space makes it highly challenging to establish a comprehensive database.

In terms of the irradiation property, ICM is used to design the irradiation hardening, embrittlement and swelling of traditional nuclear materials, primarily the steels [58–60]. So far, the application of ICM for irradiation-resistance HEAs is yet to be demonstrated, but multiple frameworks for the mechanical [49,61,62] and chemical [63,64] properties of HEAs are constructed. For instance, the high-throughput screening, multiscale modelling, and experimental validation are combined to design the light, strong, and low-cost HEAs [65]. The obtained HEA shows promise for high-temperature applications, compared with nickel-based superalloys. Recently, a performance-oriented multistage design framework for HEAs is developed, which achieves the combination of the experiment, atomic simulation, mechanical model, and machine learning [49,62]. In this framework, theoretical models are used to pre-screen the raw data, expand datasets, and constrain the results predicted from machine learning. That effectively accelerates the design process and improves the prediction accuracy. These works provide the key examples for designing the HEAs with good irradiation performance based on ICM.

3. Irradiation-controlled microstructures, properties, and damages

3.1. Damages and mechanisms

Irradiation damages are the underlying reasons for irradiation-affected microstructures and properties. The irradiation triggers high-density vacancies and interstitials, which further transform to typical irradiation-induced defects, such as DLs, SFTs, and voids. HEAs are known for the reduced irradiation damages. The density/size of irradiation-induced defects in HEAs are lower/smaller than that in conventional alloys and even the state-of-art nuclear materials, under a wide range of irradiation doses and temperatures [11,13,14]. Several unique mechanisms are proposed as the origins of the reduced irradiation damage in HEAs (Fig. 7). At the quantum-atomic scale, *ab initio* calculations reveal that the mixing of multiple elements causes a short electron mean free path, which subsequently leads to a slow energy dissipation and enhances defect recombination in the vicinity of the collision cascades [23,34]. From the point of view of energy, a remarkable overlay region between the migration energies of the vacancy and interstitial in HEAs suggests an enhanced interaction between the vacancy and interstitial [22,24]. At the nanoscale, MD simulations reveal that the motion of interstitial defect cluster transits from a long-range 1D mode to a short-range 3D mode, to enhance the point-defect recombination [17]. The severe lattice distortion induces high-density lattice vacancies to annihilate irradiation interstitials [66]. In addition, the sluggish diffusivity of HEAs also promotes the vacancy and interstitial recombination by mitigating defect migration. So far, extensive calculation works, most of them are *ab initio* calculations and MD simulations, have been made to uncover the intrinsic mechanisms of the enhanced irradiation resistance of HEAs. The union of the mechanisms from quantum to nanoscale is widely accepted by researchers, but the irradiation damage mechanisms at larger time and space scales remain unclear. For instance, the collision cascade widely concerned by MD simulations just occurs at the early stage of irradiation, while the afterward long-time (microsecond, second and year) evolution of irradiation-induced defects is beyond the scope of existing MD methods.

To date, most studies focus on the irradiation response controlled by the intrinsic characteristic of HEAs, such as the lattice distortion and sluggish diffusivity. The enhanced irradiation-defect recombination is partially explained by these intrinsic mechanisms, but the roles of microstructures in HEAs are unintentionally ignored. It remains unclear whether the effect of microstructure on irradiation damage is enhanced or weakened in HEAs. A few studies explore this issue. The MD simulations reveal that at the post-irradiation stages, the reduced dislocation mobility in HEAs suppresses the damage accumulation, and thus leads to the slower growth of dislocation clusters [36]. It is well known that the interfaces in alloys, such as GBs and phase boundaries, severe as important sinks for irradiation defects. By calculating the intensity and distribution of defect energy around GBs in the CuNiCoFe HEA, it is found that the local elemental ordering in GB greatly reduces the formation energy of the interstitial [37]. This result provides an alternative explanation for the enhanced radiation resistance for HEAs. Moreover, it suggests that the defects-absorption ability of microstructures in HEAs may be enhanced by the severe lattice distortion. The next step should identify the influences of geometrical features (like GB orientation and excess volume) and physical characteristics (like boundary energy and entropy) under the effects of lattice distortion. Note that the modulation of the microstructure is always an important strategy to improve the irradiation resistance. Therefore, more efforts are urgent to explore the possibility of enhancing irradiation performance of HEAs through tailoring microstructures.

3.2. Microstructures

Driven by the research philosophy that microstructures determine macroscopic performance, the influence of irradiation on microstructures has been a long-term research focus. Under the irradiation, the complex microstructural evolution may occur, including the dislocation network formation, GB movement, segregation, and precipitation. These microstructural phenomena are sensitive to the composition, irradiation dose and temperature.

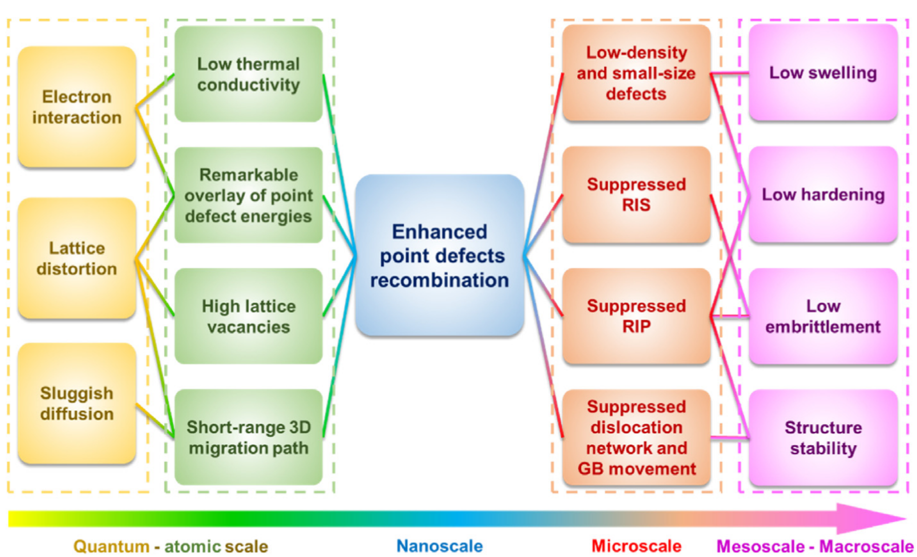

Fig. 7. Multistage irradiation response and multiscale mechanisms of HEAs. The relationship network describes multistage relationships from quantum-scale features to macroscopic performance of materials.

3.2.1. Dislocation networks

The irradiation-induced dislocation networks result from the growth of interstitial loops, which first agglomerate into DLs and then grow into dislocation networks [17]. Due to the high migration rate of interstitial atoms, the dislocation networks tend to distribute in the deeper regions. This phenomenon is suppressed by increasing the composition complexity of HEAs (Fig. 8). As revealed by the transmission electron microscopy (TEM) characterization and MD simulations, the interstitial defect motion transits from the long-range 1D mode to short-range 3D mode when the composition complexity increases [17]. That enhances the recombination of point defects in the cascade region and thereby decreases the interstitial loops for dislocation network formation. The formation of dislocation networks is enhanced at high temperature [67, 68]. A typical example is that the density and size of dislocations increase with the irradiation temperature in the $Al_{0.1}CoCrFeNi$ HEA [67]. At the critical temperature of 650 °C, the dislocation-line segments even become the domination, because the small defect clusters become unstable and absorbed. This phenomenon is triggered by the enhanced diffusivity at high temperatures [69–72], which is similar with the traditional materials. However, it is still unclear whether the temperature-enhanced dislocation networks would be suppressed, since the diffusivity of HEAs is still on debate [73–76].

In addition, the evolution of dislocation networks after irradiation is rarely studied for HEAs. In general, after irradiation, the survived defects (such as DLs and SFTs) further prevent the dislocation movement and even stimulate dislocation avalanche. DDD simulations reveal that the non-uniform distributed dislocations in irradiated materials induce locally high stresses, which leads to the significant dislocation multiplication and motion [40]. This effect may be more pronounced in HEAs since the severe lattice distortion intensifies the stress non-uniformity [38]. However, the post-irradiation evolution of dislocation networks in HEAs under the effects of irradiation-induced defects are rarely studied. The highly heterogenous stress may stimulate the localized dislocation multiplication and motion, but the long-range motion of dislocations may be inhibited by the high stress-barrier regions. This competition relationship relies on the magnitude and distribution of atomic stress field. In addition, the complex coupling effects of compositions, lattice distortions and irradiation defects on dislocation networks are also important topic, and need to be clarified using multiscale modelling and experiments.

3.2.2. GB movement

The GB movement during irradiation is driven by the local heating induced by collision cascades (Fig. 9). The irradiation-induced GB movement always accompanies with the grain growth or creep deformation, which in turn serve as the indirect evidence of the GB movement. In the nanocrystalline NiCoFeCrMn HEA, obvious grain growth (grain size increases from 28 nm to 65 nm) occurs when the irradiation temperature increases from 293 K to 753 K. It indicates the irradiation-induced GB movement [77]. In the refractory HEAs (RHEAs), the GB movement is strongly suppressed even at high temperatures [25], suggesting the good structure stability during irradiation. Note that the RHEAs are natural with high thermal stability, since they are composing of refractory elements. Therefore, the high GB stability is mainly attribute to the intrinsic thermal-stability of RHEAs. The contributions of other factors, such as the irradiation-induced defects, are not clear for HEAs. In traditional alloys, the high-density point defects generated by irradiation accelerate the GB movement due to the enhanced point-defects flow. In this case, the density and flowability of irradiation-induced defects in HEAs are the critical factors. Because the recombination of irradiation-induced defects is enhanced, and the diffusivity is slow in HEAs [73,78–80], it is logical to deduce that the irradiation-induced GB movement would be less pronounced compared than that in traditional alloys.

Currently, the direct observation of the irradiation-induced GB movement is not yet realized for HEAs but already for dilute alloys. *In-situ* TEM reveals that the GB migration occurs by absorbing irradiation-induced vacancies and voids, especially at elevated temperatures and high irradiation doses [82–84]. Combining high-angle annular dark field

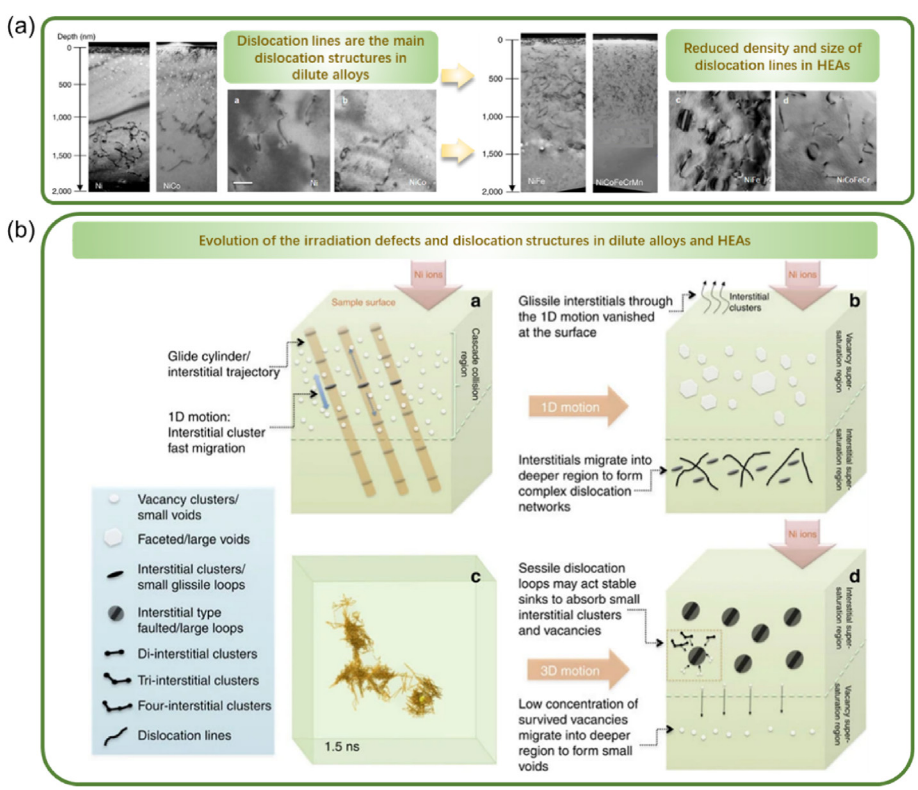

Fig. 8. Irradiation-induced dislocation networks [17]. (a) Distribution of dislocations and DLs in Ni and Ni-containing HEAs. (b) Schematic illustration of 1D and 3D motions of interstitial clusters under ion irradiation.

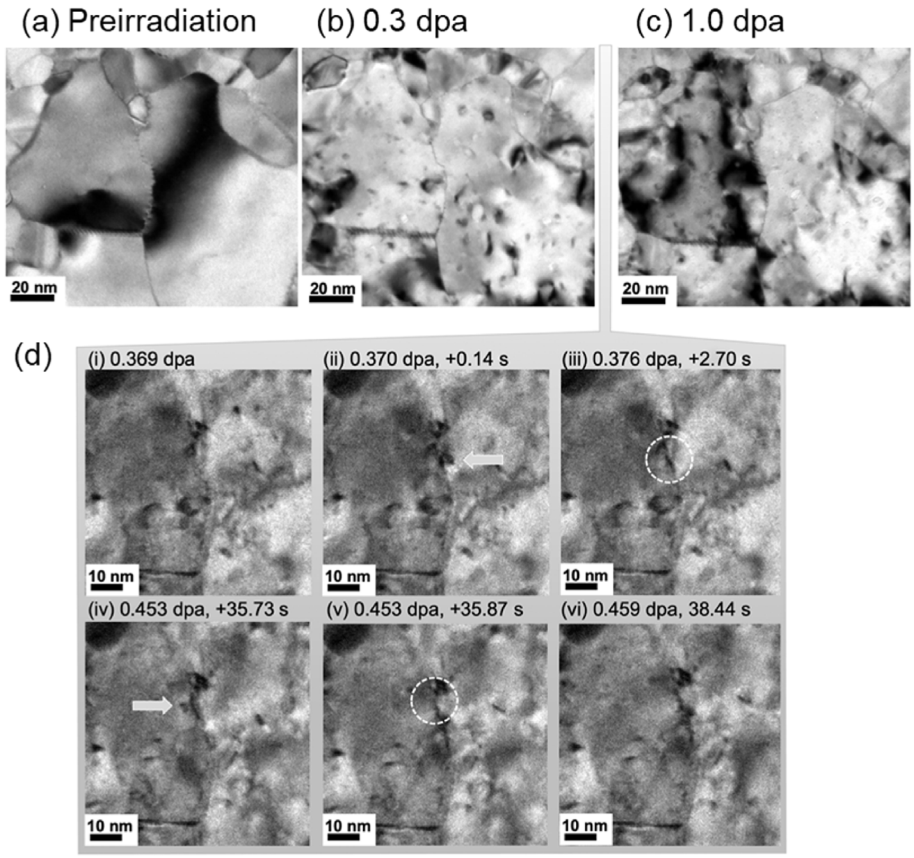

Fig. 9. Irradiation-induced GB movement [81]. Evolution of GB during irradiation under (a) pre-irradiation state, (b) 0.3 dpa irradiation state, and (c) 1.0 dpa irradiation state. (d) Series of still frames taken from in situ TEM.

- scanning transmission electron microscopy (HAADF-STEM) with MD simulations, a recent study reveals that the GB motion is driven by the local heating, while the ion strike just induces GB roughening [81]. The two results make the irradiation-induced GB motion in HEAs difficult to predict. In HEAs, high defect recombination reduces survived irradiation defects, which suppresses the GB motion; However, the low thermal conductivity allows for high local heating, which may enhance the GB motion. Experiments and MD simulations reveal that the GB roughening always causes a decrease in the GB migration barrier [85,86]. This trend indicates that the GB motion is easy to be driven by the irradiation-induced thermal stress. Therefore, more effort is still required to resolve this contradiction.

3.2.3. Segregation

Radiation-induced segregation (RIS) is prevailed in HEAs. On one hand, irradiation-induced high-density point defects tend to flow to pre-existing defect sinks, which are accompanied with the flux of solutes. On the other hand, the locally high temperature around the cascade regions provides a strong driven force for the flow of defects and solutes [68]. For HEAs, both the single-element segregation [87–89] and multielement co-segregation [90] after irradiation are experimentally observed. A typical example is the irradiated FeNiMnCr HEA, in which the enrichment of Ni and depletion of Mn around GBs are observed [89]. Such segregation occurs at very early stages of radiation damage, as shown in the NiCoFeCr HEAs [88]. The integrate results from positron annihilation spectroscopy and MD simulations show that the irradiation-induced vacancies are enriched with Ni elements, especially for the alloys with higher entropy. Such fast segregation derives from not only the irradiation-heat driven diffusion, but also the strong bonding tendency between vacancy and Ni compared with other elements. Ab initio calculations of the defect properties in NiCoCr and NiCoCrFe HEAs reveal that the vacancy formation energy decreases as more Ni atoms surround the vacancy, while more Co, Cr and Fe elements would increase the vacancy formation energy [22]. These results highlight that any stages of irradiation response should consider the influence of RIS in HEAs. In terms of co-segregation, atom probe tomography (APT) and STEM-EDS detect the co-segregation of Co and Ni at high-angle GBs in the irradiated CoCrFeNiMn and $Al_{0.1}$CoCrFeNi HEAs [67,91], while the enhanced segregation of Cr and V after irradiation is observed in WTaCrV HEAs (Fig. 10) [25]. The types of co-segregation elements are determined by the positive mixing enthalpies between the considered elements, as revealed by *ab initio* calculations and cluster expansion methodology [25].

The RIS in HEAs is controlled by the bias vacancy-solute-based inverse Kirkendall effect mechanism [91]. The diffusivity differences determine the segregation and depletion of specific elements at sinks. The fastest diffusive element depletes at the point-defect sinks, while the slowest diffusive element tends to enrich the sinks. This conclusion is valid for most experiments [89,92]. For example, in the irradiated CoCrFeNiMn HEA, the fastest diffuser (Mn) depletes at GBs while the slowest diffuser (Co) enriches [91,92]. In the WTaCrV HEA, Ta exhibits the lowest diffusion barrier [24], leading to the Ta depletion in the irradiated sample [25]. Since the RIS mainly occurs at sinks (mainly GBs), the physical characteristics of sinks plays significant roles in degree of segregation. For the nanotwin boundaries in $Fe_{30}Cr_{25}Ni_{20}Co_{15}Mn_{10}$ HEA, only slight segregation of Co and Ni is observed [93], because the excess energy and volume of twin boundaries are very small. Accordingly, the low-angle GBs would exhibit weak RIS because of their low excess energies and volume. However, the detailed relationships between GB properties and RIS in HEAs are still unstudied, especially under the complex effects of lattice distortion and sluggish diffusion hypothesis.

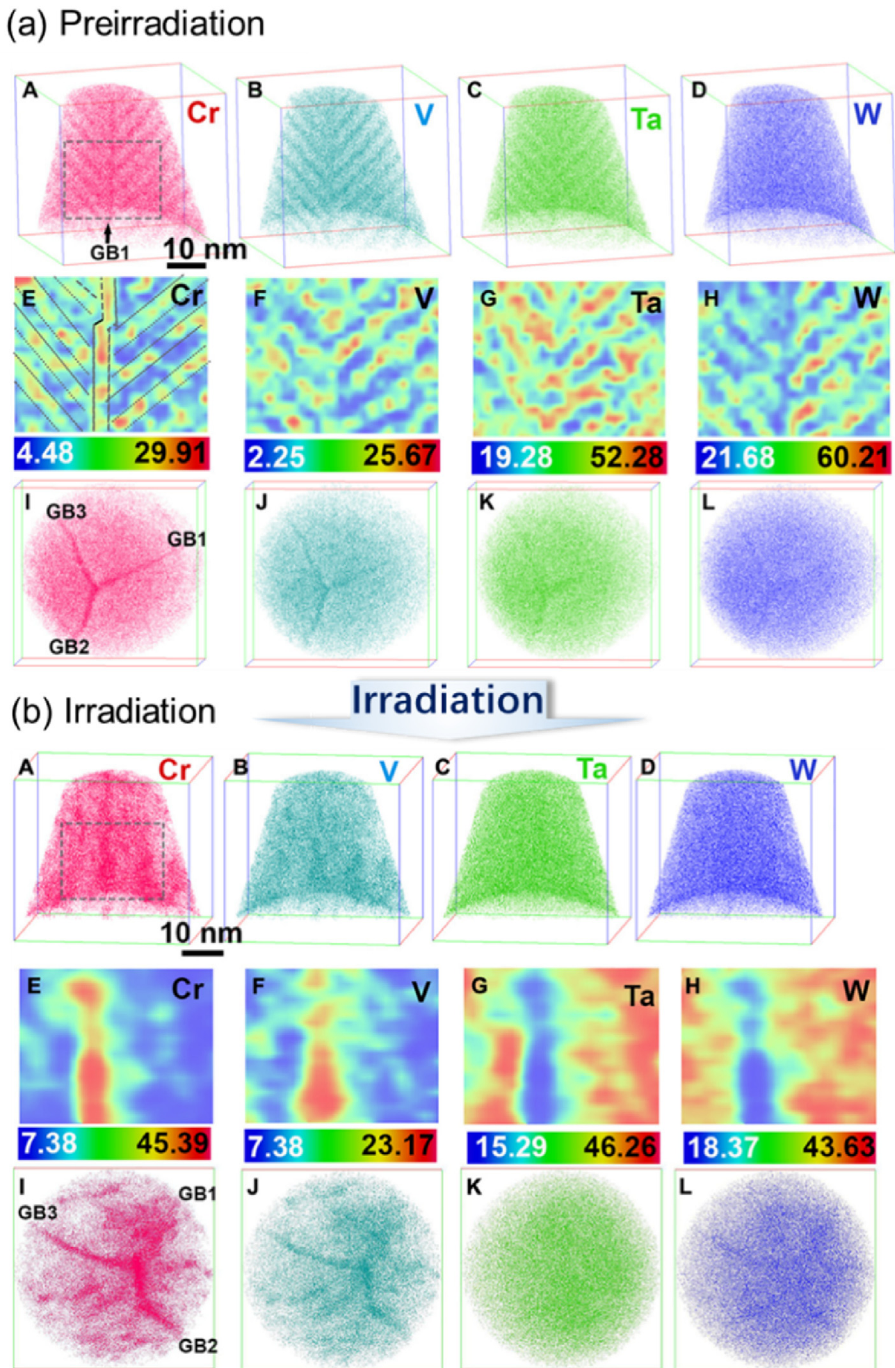

Fig. 10. Irradiation-induced segregation. APT analysis of the WTaCrV HEA (a) before irradiation, and (b) after irradiation to 8 dpa with 3 MeV Cu^+ at 1050 K. From Ref. [25].

3.2.4. Precipitation

The RIS of elements further induces precipitation, once the local concentration exceeds the solubility limit. Early studies show that HEAs exhibit great phase stability under irradiation. Typical examples include the Cantor alloy and its subsystems, in which the FCC solid solution remains the main phase after irradiation at wide-range temperatures [11]. However, irradiation indeed induces phase instability, since the transformation from the L12 to B2 phases is detected after irradiation [94]. The radiation-induced precipitation (RIP) enriched with Cr and V in the W-based RHEA is also observed (Fig. 11) [25]. Improving the irradiation temperature promotes RIP in HEAs, attributing to the enhanced diffusion at high temperature. The representative study of the temperature effect can be seen in $Al_{0.3}$CoCrFeNi HEA [68]. The precipitation of (Ni, Al)-enriched clusters and $L1_2$ phases are suppressed at low irradiation temperature (250 °C–500 °C), while the precipitation of B2 precipitates are accelerated at high temperature (650 °C). The RIP is thermodynamically controlled by the elemental diffusivity and mixing enthalpy, whereas the former controls the composition and the later governs the lattice structure. Specifically, the positive and negative enthalpies of mixing values indicate a tendency for segregation or ordering, respectively. For example, the $L1_0$-type NiMn precipitates are formed in the radiated Cantor alloy due to the negative enthalpy between Ni and Mn [94]. The negative Cr–V mixing enthalpy triggers the precipitation of Cr–V-enriched particles in irradiated WTaCrV HEAs [25]. Here, it is worth to note that the mixing enthalpy is not only

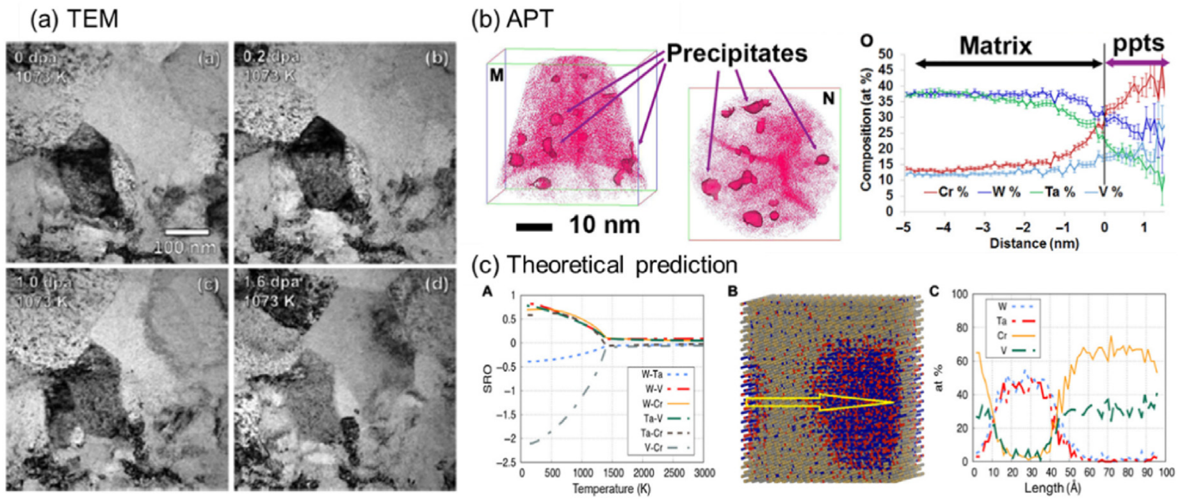

Fig. 11. Irradiation-induced precipitation. (a) The enhanced precipitation (black spot formation) in irradiated WTaCrV HEA. (b) The Cr–V-rich precipitates inside grains and compositions. (c) Theoretical predictions of the atomic configurations of precipitates. From Ref. [25]. © The Authors, some rights reserved; exclusive licensee AAAS. Distributed under a CC BY-NC 4.0 license http://creativecommons.org/licenses/by-nc/4.0/". Reprinted with permission from AAAS.

affected by the chemical bonding, but also the difference of atomic size. For HEAs, the complex chemical situation and significant atomic-size misfit change the mixing enthalpies compared with traditional alloys. Therefore, the RIP observed in dilute alloys may be invalid for HEAs. That means the mixing-enthalpy-based prediction of RIP in HEAs need to be revaluated using theories and calculations [25].

3.3. Properties

Changes of material properties due to irradiation are the ultimate focus of research. The irradiation-induced swelling, hardening, and embrittlement receive much attention (Fig. 12d), as they severely weaken the potential of materials as the structure member of nuclear reactors.

3.3.1. Swelling

The radiation-induced swelling is triggered by the accumulation of radiation-induced voids. Logically, low swelling is realized by decreasing the density and size of voids. In general, HEAs exhibit high swelling resistance even compared with advanced irradiation-resistant steels (Fig. 12a), because the high defect recombination rate suppresses void formation. Representative examples include the CrCoFeNiMn HEA [95] and HfNbTaTiZr RHEAs [102].

The swelling resistance is sensitive to both the alloying degree and element type [95]. For NiCoCrFeMn systems, the swelling resistance is ranked in the order Ni < NiCo < NiFe < NiCoCrFe < NiCoFe < NiCoCrFeMn. The addition of Fe is more effective to reduce swelling than Co, leading to the high swelling resistance of NiFe compared to NiCo,

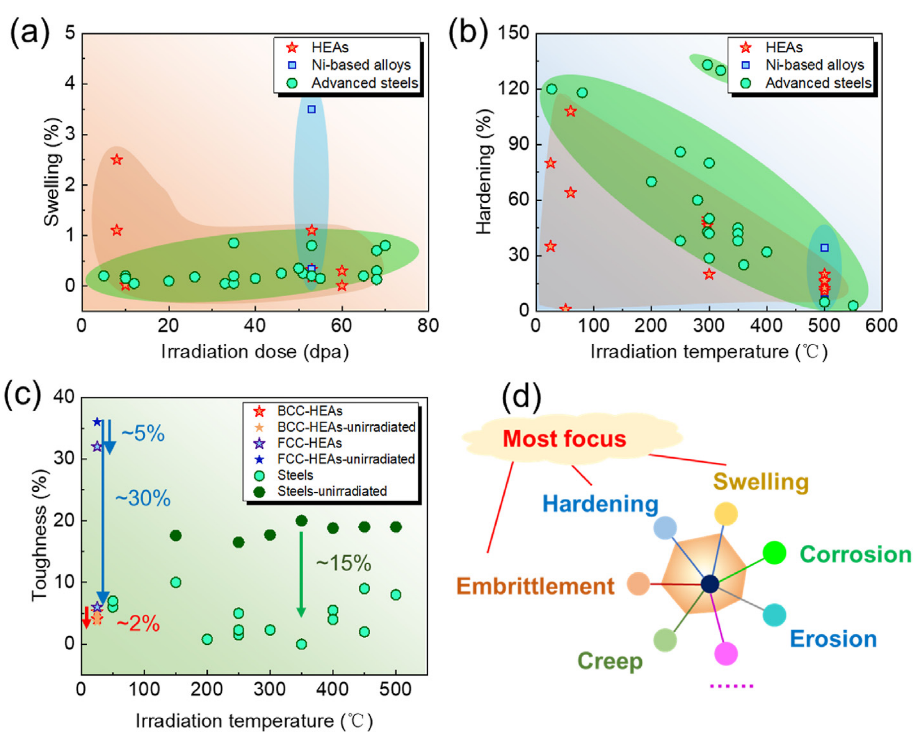

Fig. 12. Irradiation-induced properties of HEAs. The properties of (a) swelling [14,95–97], (b) hardening [14,15,89,93,95,98,99], and (c) embrittlement [98,100,101] are presented. (d) Attention to different irradiation-induced properties of HEAs.

NiCoCr, and NiCoFe. The influence of pre-existing defect sinks on swelling is important and elusive for HEAs. The nanocrystalline $Al_{1.5}CoCrFeNi$ HEA with high-density GBs displays excellent swelling resistance compared to the coarse-grained counterpart [96], but the abnormally enhanced swelling in the NiCoFeCrPd HEA with high-density dislocations are also observed [103]. Further investigation reveals that the severe lattice distortion in the NiCoFeCrPd HEA over-enhances the interstitial absorption capacity of dislocations. This trend leads to the survival of numerous vacancies due to the lack of interstitial atoms for recombination. Increasing the irradiation temperature also promotes the swelling of HEAs, because the interstitial atoms escape to surface or deep regions that far away from survived vacancies [104]. These works partially reveal the influence of specific elements, lattice distortion, temperature, and microstructures on the swelling of several HEAs. However, coupling effects of these factors on the swelling are still unclear, especially the severe lattice distortion that is unique for the HEA.

3.3.2. Hardening

The irradiation hardening origins from the formation of high-density defect clusters, especially the DLs, SFTs, and voids. These clusters strongly inhibit the dislocation motion to improve the hardness. For HEAs, the hardening is weak due to suppressed irradiation defects (Fig. 12b). The irradiated HfTaTiVZr RHEA presents only 13% hardening rate compared to 50% hardening for the advanced SS304 steel under identical irradiation conditions, attributing to the reduced mobility of point defects and self-healing ability in the RHEA [15]. Via precisely tailoring the composition and post-irradiation annealing, non-hardening is even achieved for the HEA. The $Ti_2ZrHfV_{0.5}Mo_{0.2}$ RHEA presents scarce hardening and anomalous lattice shrinkage after high-dose He^+ irradiation, attributing to the severe lattice distortion that produces high-density lattice vacancies/defects to capture He atoms [66]. The significant hardening of the NiFeMnCr HEA induced by neutron-irradiation is eliminated by 650 °C annealing, indicating the promise of HEAs for high-temperature neutron irradiation applications [98]. Overall, the BCC RHEA exhibit higher irradiation-hardening resistance compared with the FCC HEA. On one hand, the intrinsic hardness of BCC phases is generally higher than that of FCC phases, which dilute the additional hardness cause by irradiation; on the other hand, the large-atomic-size refractory elements (like V and Hf) exacerbates the lattice distortion, thus suppress irradiation damage.

In addition to reduce irradiation defects, low hardening can be realized by activating extra softening mechanisms. The TiZrNbHfTa RHEA exhibits only 13.9% hardening while retaining 4.5% elongation, because nanoscale He bubbles weaken GBs to activate the GB-gliding mechanism [101]. The hardening can be further suppressed by increasing the irradiation temperature, which transforms much DLs into dislocation lines to induce softening [89]. These works suggest an alternative strategy to reduce irradiation hardening, but the application of this strategy is limited by the viable softening mechanisms in alloys. Simulations and experiments uncover the occurrence of SFs, twining, phase transformation and amorphization in HEAs [105–108], especially under extreme conditions. Therefore, exact for GB-mediated mechanisms, more softening mechanisms in HEAs are expected since complicate microstructures are easy to be activated [4,5].

3.3.3. Embrittlement

Irradiation-induced embrittlement is a key factor affecting the safe service of nuclear materials. Experiments reveal that RIS and RIP are the main reasons for embrittlement. Based on this logic, HEAs are expected to exhibit high embrittlement resistance since the high defect recombination naturally suppresses RIS and RIP. This extrapolation is verified by several HEAs (Fig. 12c), such as the $V_{2.5}Cr_{1.2}WMoCo_{0.04}$ [16] and $Ti_2ZrHfV_{0.5}Mo_{0.2}$ [66]. Particularly, the $Ti_2ZrHfV_{0.5}Mo_{0.2}$ HEA exhibits low helium-ion irradiation embrittlement, attributing to the highly concentrated inherent vacancy defects that effectively capture the helium atoms [66]. The enrichment of helium atoms at vacancies not only reduces the distortion around the vacancy defects and thus the lattice expansion, but also suppresses the formation of intergranular helium bubbles that always leads to embrittlement. These results suggest that high helium-ion irradiation resistance can be realized via increasing the intrinsic lattice defects in HEAs.

The basic step to control the embrittlement of HEAs is to tailor compositions. Dangerous elements that always induce embrittlement should be avoided in the first place, such as H for almost all HEAs [13] and Ti/Cr for the V-based HEAs [12]. Specifically, the reduction of the interstitial solute is also necessary for the V-based HEAs [12]. Interestingly, the RIS with a moderate segregator may induce abnormal toughening. When the moderate amount of H enriches at GBs in FeCrNiMnCo HEA, the toughness increases abnormally because the H atom promotes the formation of SFs and nanotwins [109]. This trend also benefits from the low SF energy of HEAs. To minimize embrittlement, brittle phases like alpha and Laves phases should be strongly avoided. At present, only a few studies have addressed the embrittlement of HEAs, and further study need to draw more on the embrittlement results of the irradiated steel.

4. Conclusions

Multiscale-modelling methods successfully explore the irradiation responses and underlying mechanisms of HEAs. The reduction of irradiation-induced swelling, hardening, and embrittlement, as well as the excellent structure stability, which derives from the suppression of microstructure evolution, are further attributed to the enhanced defect recombination. At the quantum scale, the low thermal conductivity due to the constrained electron motion and the remarkable overlay region of migration energy between point defects strengthen the defect interaction. At nanoscale, severe lattice distortion induces the short-range 3D mode of the interstitial movement and high-density lattice vacancies also enhance the defect recombination. The reduced dislocation mobility and strong interstitial-absorption of GBs in HEAs further suppress the growth of irradiation defects. The synergy of these multiscale mechanisms reduces the density and size of voids to reduce swelling, slows down the growth of DLs and SFTs to suppress hardening, weakens the RIS and RIP to suppress embrittlement, and inhibits the dislocation-networks formation and GB movement to lessen structure inability.

Most works focus on the influence of material characteristics (compositions and microstructures) and irradiation conditions (doses and temperatures) on irradiation responses of HEAs. However, a comprehensive understanding of the roles of composition fluctuations, severe lattice distortion, and sluggish diffusion on irradiation response in HEAs is still scarce. To address this critical issue, advanced multiscale and cross-scale calculation strategies are urgent, because they can finely control and accurately evaluate each influencing factor. Meanwhile, high-throughput methods combined with machine learning provide effective and efficient tools to accelerate the exploration and further design the irradiation performance of HEAs. The combination of multiscale methods and big-data technologies open new doors for exploring the advanced irradiation-resistant HEAs.

5. Perspectives

So far, the excellent irradiation resistance and broad development prospects of HEAs have been widely recognized. Prior experiments and simulations have preliminarily explored the nano- and microscopic roots of the irradiation resistance of HEA. However, the coupling effects of complex intrinsic properties (composition, distorted lattice, and microstructures) and irradiation conditions (temperature, pressure, and radiation source) on the irradiation response of HEAs remain unclear. That limits the development of physical-origin-driven design method, thus leading to the slow development of irradiation-resistant properties of HEAs. To address this problem, the application of multiscale modelling methodology in irradiation needs to be further extended. Attention needs to be paid to the following future directions emphasizing multiscale modelling in HEAs.

1) Multiscale simulations that more closely match actual irradiation conditions.

That mainly includes the irradiation simulations under the coupling operation of high temperature and high pressure, different radiation sources (ion, neutron, and electron irradiations), and multiple time scales (picoseconds, seconds, months, and years). To achieve that, advanced simulation methodologies need to be applied, such as the accelerate MD [110], the lattice distortion dependent DDD [38], and the hierarchical multiscale CPFEM [42].

2) Physical-origins-dependent theoretical models for irradiation response of HEAs.

The theories are based on the irradiation damage and deformation mechanisms revealed by experiments and multiscale simulations. Meanwhile, the intrinsic characteristics of HEAs should be considered, such as the lattice distortion and chemical heterogeneity.

3) Multiscale design framework for optimizing composition and microstructure of high irradiation-resistant HEAs.

The cores of the framework are the physical-origins-dependent theoretical model and machine learning techniques [49,62]. The machine learning model should cover the intrinsic characteristics of HEA and key parameters representing irradiation properties, and the theoretical model helps to pre-screen, expand, and constrain the database. To construct the database for machine learning, high-throughput experiments and calculations are required [51,62,111].

Declaration of competing interest

The authors declare that they have no known competing financial interests or personal relationships that could have appeared to influence the work reported in this paper.

Acknowledgement

The authors would like to deeply appreciate the supports from National Natural Science Foundation of China (U2267252, 12172123, and 12072109), Natural Science Foundation of Hunan Province (2022JJ20001 and 2021JJ40032), The science and technology innovation Program of Hunan Province (2022RC1200), and Natural Science Foundation of Changsha City (kq2202139). PKL very much appreciates the support from the National Science Foundation (DMR-1611180 and 1809640).

References

[1] C.B.A. Forty, P.J. Karditsas, Uses of zirconium alloys in fusion applications, J. Nucl. Mater. 283 (2000) 607–610.
[2] J. Knaster, A. Moeslang, T. Muroga, Materials research for fusion, Nat. Phys. 12 (2016) 424–434.
[3] S.J. Zinkle, J.T. Busby, Structural materials for fission & fusion energy, Mater. Today 12 (2009) 12–19.
[4] E.P. George, D. Raabe, R.O. Ritchie, High-entropy alloys, Nat. Rev. Mater. 4 (2019) 515–534.
[5] D.B. Miracle, O.N. Senkov, A critical review of high entropy alloys and related concepts, Acta Mater. 122 (2017) 448–511.
[6] Y. Zhang, T.T. Zuo, Z. Tang, M.C. Gao, K.A. Dahmen, P.K. Liaw, Z.P. Lu, Microstructures and properties of high-entropy alloys, Prog. Mater. Sci. 61 (2014) 1–93.
[7] Q.S. Pan, L.X. Zhang, R. Feng, Q.H. Lu, K. An, A.C. Chuang, J.D. Poplawsky, P.K. Liaw, L. Lu, Gradient cell-structured high-entropy alloy with exceptional strength and ductility, Science 374 (2021) 984–989.
[8] P.J. Shi, R.G. Li, Y. Li, Y.B. Wen, Y.B. Zhong, W.L. Ren, Z. Shen, T.X. Zheng, J.C. Peng, X.L. Liang, P.F. Hu, N. Min, Y. Zhang, Y. Ren, P.K. Liaw, D. Raabe, Y.D. Wang, Hierarchical crack buffering triples ductility in eutectic herringbone high-entropy alloys, Science 373 (2021) 912–918.
[9] Z.J. Shi, Z.B. Wang, X.D. Wang, S. Zhang, Y.G. Zheng, Effect of thermally induced B2 phase on the corrosion behavior of an Al0.3CoCrFeNi high entropy alloy, J. Alloys Compd. 903 (2022), 163886.
[10] I. Baker, Interstitial strengthening in f.c.c. metals and alloys, Adv. Powder Mater. 1 (2022), 100034.
[11] Z.R. Zhang, D.E.J. Armstrong, P.S. Grant, The effects of irradiation on CrMnFeCoNi high-entropy alloy and its derivatives, Prog. Mater. Sci. 123 (2022), 100807.
[12] P.J. Barron, A.W. Carruthers, J.W. Fellowes, N.G. Jones, H. Dawson, E.J. Pickering, Towards V-based high-entropy alloys for nuclear fusion applications, Scripta Mater. 176 (2020) 12–16.
[13] E.J. Pickering, A.W. Carruthers, P.J. Barron, S.C. Middleburgh, D.E.J. Armstrong, A.S. Gandy, High-entropy alloys for advanced nuclear applications, Entropy-Switz 23 (2021) 98.
[14] A.O. Moghaddam, A. Cabot, E.A. Trofimov, Does the pathway for development of next generation nuclear materials straightly go through high-entropy materials? Int J Refract Met H 97 (2021), 105504.
[15] M. Sadeghilaridjani, A. Ayyagari, S. Muskeri, V. Hasannaeimi, R. Salloom, W.Y. Chen, S. Mukherjee, Ion irradiation response and mechanical behavior of reduced activity high entropy alloy, J. Nucl. Mater. 529 (2020), 151955.
[16] D. Patel, M.D. Richardson, B. Jim, S. Akhmadaliev, R. Goodall, A.S. Gandy, Radiation damage tolerance of a novel metastable refractory high entropy alloy V2.5Cr1.2WMoCo0.04, J. Nucl. Mater. 531 (2020), 152005.
[17] C.Y. Lu, L.L. Niu, N.J. Chen, K. Jin, T.N. Yang, P.Y. Xiu, Y.W. Zhang, F. Gao, H.B. Bei, S. Shi, M.R. He, I.M. Robertson, W.J. Weber, L.M. Wang, Enhancing radiation tolerance by controlling defect mobility and migration pathways in multicomponent single-phase alloys, Nat. Commun. 7 (2016) 1–8.
[18] C. Niu, A.J. Zaddach, A.A. Oni, X. Sang, J.W. Hurt, J.M. LeBeau, C.C. Koch, D.L. Irving, Spin-driven ordering of Cr in the equiatomic high entropy alloy NiFeCrCo, Appl. Phys. Lett. 106 (2015), 161906.
[19] D.J.M. King, P.A. Burr, E.G. Obbard, S.C. Middleburgh, DFT study of the hexagonal high-entropy alloy fission product system, J. Nucl. Mater. 488 (2017) 70–74.
[20] Z.Y. Leong, J.S. Wrobel, S.L. Dudarev, R. Goodall, I. Todd, N.M. Duc, The effect of electronic structure on the phases present in high entropy alloys, Sci. Rep. 7 (2017), 39803.
[21] D.J.M. King, S.T.Y. Cheung, S.A. Humphry-Baker, C. Parkin, A. Couet, M.B. Cortie, G.R. Lumpkin, S.C. Middleburgh, A.J. Knowles, High temperature, low neutron cross-section high-entropy alloys in the Nb–Ti–V–Zr system, Acta Mater. 166 (2019) 435–446.
[22] S.J. Zhao, T. Egami, G.M. Stocks, Y.W. Zhang, Effect of d electrons on defect properties in equiatomic NiCoCr and NiCoFeCr concentrated solid solution alloys, Phys. Rev. Mater. 2 (2018), 013602.
[23] Y.W. Zhang, G.M. Stocks, K. Jin, C.Y. Lu, H.B. Bei, B.C. Sales, L.M. Wang, L.K. Beland, R.E. Stoller, G.D. Samolyuk, M. Caro, A. Caro, W.J. Weber, Influence of chemical disorder on energy dissipation and defect evolution in concentrated solid solution alloys, Nat. Commun. 6 (2015) 8736.
[24] S.J. Zhao, Defect properties in a VTaCrW equiatomic high entropy alloy (HEA) with the body centered cubic (bcc) structure, J. Mater. Sci. Technol. 44 (2020) 133–139.
[25] O. El-Atwani, N. Li, M. Li, A. Devaraj, J.K.S. Baldwin, M.M. Schneider, D. Sobieraj, J.S. Wrobel, D. Nguyen-Manh, S.A. Maloy, E. Martinez, Outstanding radiation resistance of tungsten-based high-entropy alloys, Sci. Adv. 5 (2019), eaav2002.
[26] Y.W. Zhang, G.M. Stocks, K. Jin, C.Y. Lu, H.B. Bei, B.C. Sales, L.M. Wang, L.K. Beland, R.E. Stoller, G.D. Samolyuk, M. Caro, A. Caro, W.J. Weber, Influence of chemical disorder on energy dissipation and defect evolution in concentrated solid solution alloys, Nat. Commun. 6 (2015) 1–9.
[27] S. Plimpton, Fast parallel algorithms for short-range molecular dynamics, J. Comput. Phys. 117 (1995) 1–19.
[28] X.W. Zhou, R.A. Johnson, H.N.G. Wadley, Misfit-energy-increasing dislocations in vapor-deposited CoFe/NiFe multilayers, Phys. Rev. B 69 (2004), 144113.
[29] D. Farkas, A. Caro, Model interatomic potentials and lattice strain in a high-entropy alloy, J. Mater. Res. 33 (2018) 3218–3225.
[30] W.M. Choi, Y. Kim, D. Seol, B.J. Lee, Modified embedded-atom method interatomic potentials for the Co–Cr, Co–Fe, Co–Mn, Cr–Mn and Mn–Ni binary systems, Comput. Mater. Sci. 130 (2017) 121–129.
[31] X.S. Huang, L.H. Liu, X.B. Duan, W.B. Liao, J.J. Huang, H.B. Sun, C.Y. Yu, Atomistic simulation of chemical short-range order in HfNbTaZr high entropy alloy based on a newly-developed interatomic potential, Mater. Des. 202 (2021), 109560.
[32] Z.N. Wang, J. Li, Q.H. Fang, B. Liu, L.C. Zhang, Investigation into nanoscratching mechanical response of AlCrCuFeNi high-entropy alloys using atomic simulations, Appl. Surf. Sci. 416 (2017) 470–481.
[33] A. Sharma, S.A. Deshmukh, P.K. Liaw, G. Balasubramanian, Crystallization kinetics in AlxCrCoFeNi ($0 <= x <= 40$) high-entropy alloys, Scripta Mater. 141 (2017) 54–57.
[34] Y.P. Lin, T.F. Yang, L. Lang, C. Shan, H.Q. Deng, W.Y. Hu, F. Gao, Enhanced radiation tolerance of the Ni–Co–Cr–Fe high-entropy alloy as revealed from primary damage, Acta Mater. 196 (2020) 133–143.
[35] J. Peng, S.Y. Cui, Y.Y. Tian, Q.H. Fang, J. Li, P.K. Liaw, Effects of grain boundary on irradiation-induced zero-dimensional defects in an irradiated copper, Appl Math Mech-Engl. 43 (2022) 233–246.
[36] F. Granberg, K. Nordlund, M.W. Ullah, K. Jin, C. Lu, H. Bei, L.M. Wang, F. Djurabekova, W.J. Weber, Y. Zhang, Mechanism of radiation damage reduction in equiatomic multicomponent single phase alloys, Phys. Rev. Lett. 116 (2016), 135504.

[37] S.J. Zhao, Effects of local elemental ordering on defect-grain boundary interactions in high-entropy alloys, J. Alloys Compd. 887 (2021), 161314.
[38] J. Li, Y. Chen, Q. He, X. Xu, H. Wang, C. Jiang, B. Liu, Q. Fang, Y. Liu, Y. Yang, Heterogeneous lattice strain strengthening in severely distorted crystalline solids, Proc. Natl. Acad. Sci. USA 119 (2022), e2200607119.
[39] Y.N. Cui, N. Ghoniem, G. Po, Plasticity of irradiated materials at the nano and micro-scales, J. Nucl. Mater. 546 (2021), 152746.
[40] Y.A. Cui, G. Po, N. Ghoniem, Does irradiation enhance or inhibit strain bursts at the submicron scale? Acta Mater. 132 (2017) 285–297.
[41] Y.A. Cui, G. Po, N. Ghoniem, Size-tuned plastic flow localization in irradiated materials at the submicron scale, Phys. Rev. Lett. 120 (2018), 215501.
[42] Q.H. Fang, W.Z. Lu, Y. Chen, H. Feng, P.K. Liaw, J. Li, Hierarchical multiscale crystal plasticity framework for plasticity and strain hardening of multi-principal element alloys, J. Mech. Phys. Solid. 169 (2022), 105067.
[43] X.C. Lu, J.F. Zhao, C. Yu, Z.M. Li, Q.H. Kan, G.Z. Kang, X. Zhang, Cyclic plasticity of an interstitial high-entropy alloy: Experiments, crystal plasticity modeling, and simulations, J. Mech. Phys. Solid. 142 (2020), 103971.
[44] A. Patra, D.L. McDowell, Crystal plasticity investigation of the microstructural factors influencing dislocation channeling in a model irradiated bcc material, Acta Mater. 110 (2016) 364–376.
[45] A. Patra, D.L. McDowell, Continuum modeling of localized deformation in irradiated bcc materials, J. Nucl. Mater. 432 (2013) 414–427.
[46] Z.J. Li, Z.L. Liu, Z. Zhuang, Y.A. Cui, Temperature dependent deformation localization in irradiated tungsten, Int. J. Plast. 146 (2021), 103077.
[47] X.Z. Xiao, D.K. Song, J.M. Xue, H.J. Chu, H.L. Duan, A size-dependent tensorial plasticity model for FCC single crystal with irradiation, Int. J. Plast. 65 (2015) 152–167.
[48] J. Gao, J. Zhong, G. Liu, S. Yang, B. Song, L. Zhang, Z. Liu, A machine learning accelerated distributed task management system (Malac-Distmas) and its application in high-throughput CALPHAD computation aiming at efficient alloy design, Adv. Powder Mater. 1 (2022), 100005.
[49] J. Li, B.B. Xie, L. Li, B. Liu, Y. Liu, D. Shaysultanov, Q.H. Fang, N. Stepanov, P.K. Liaw, Performance-oriented multistage design for multi-principal element alloys with low cost yet high efficiency, Mater. Horiz. 9 (2022) 1518–1525.
[50] P. Raccuglia, K.C. Elbert, P.D.F. Adler, C. Falk, M.B. Wenny, A. Mollo, M. Zeller, S.A. Friedler, J. Schrier, A.J. Norquist, Machine-learning-assisted materials discovery using failed experiments, Nature 533 (2016) 73–76.
[51] F. Liu, Z.X. Wang, Z. Wang, J. Zhong, L. Zhao, L. Jiang, R.H. Zhou, Y. Liu, L. Huang, L.M. Tan, Y.J. Tian, H. Zheng, Q.H. Fang, L.J. Zhang, L.N. Zhang, H. Wu, L.C. Bai, K. Zhou, High-throughput method-accelerated design of Ni-based superalloys, Adv. Funct. Mater. 32 (2022), 2109367.
[52] S.J. Zhao, Application of machine learning in understanding the irradiation damage mechanism of high-entropy materials, J. Nucl. Mater. 559 (2022), 153462.
[53] N. Castin, L. Malerba, Calculation of proper energy barriers for atomistic kinetic Monte Carlo simulations on rigid lattice with chemical and strain field long-range effects using artificial neural networks, J. Chem. Phys. 132 (2010), 074507.
[54] M.I. Pascuet, N. Castin, C.S. Becquart, L. Malerba, Stability and mobility of Cu-vacancy clusters in Fe–Cu alloys: A computational study based on the use of artificial neural networks for energy barrier calculations, J. Nucl. Mater. 412 (2011) 106–115.
[55] N. Castin, L. Messina, C. Domain, R.C. Pasianot, P. Olsson, Improved atomistic Monte Carlo models based on *ab-initio*-trained neural networks: application to FeCu and FeCr alloys, Phys. Rev. B 95 (2017), 214117.
[56] L. Messina, N. Castin, C. Domain, P. Olsson, Introducing ab initio based neural networks for transition-rate prediction in kinetic Monte Carlo simulations, Phys. Rev. B 95 (2017), 064112.
[57] A. Manzoor, G. Arora, B. Jerome, N. Linton, B. Norman, D.S. Aidhy, Machine learning based methodology to predict point defect energies in multi-principal element alloys, Front. Mater. 8 (2021) 129.
[58] J. Mathew, D. Parfitt, K. Wilford, N. Riddle, M. Alamaniotis, A. Chroneos, M.E. Fitzpatrick, Reactor pressure vessel embrittlement: Insights from neural network modelling, J. Nucl. Mater. 502 (2018) 311–322.
[59] R. Kemp, G.A. Cottrell, H.K.D.H. Bhadeshia, G.R. Odette, T. Yamamoto, H. Kishimoto, Neural-network analysis of irradiation hardening in low-activation steels, J. Nucl. Mater. 348 (2006) 311–328.
[60] M.M. Jin, P.H. Cao, M.P. Short, Predicting the onset of void swelling in irradiated metals with machine learning, J. Nucl. Mater. 523 (2019) 189–197.
[61] C. Wen, C.X. Wang, Y. Zhang, S. Antonov, D.Z. Xue, T. Lookman, Y.J. Su, Modeling solid solution strengthening in high entropy alloys using machine learning, Acta Mater. 212 (2021), 116917.
[62] J. Li, B.B. Xie, Q.H. Fang, B. Liu, Y. Liu, P.K. Liaw, High-throughput simulation combined machine learning search for optimum elemental composition in medium entropy alloy, J. Mater. Sci. Technol. 68 (2021) 70–75.
[63] P. Lu, J.E. Saal, G.B. Olson, T.S. Li, O.J. Swanson, G.S. Frankel, A.Y. Gerard, K.F. Quiambao, J.R. Scully, Computational materials design of a corrosion resistant high entropy alloy for harsh environments, Scripta Mater. 153 (2018) 19–22.
[64] B.X. Wei, J. Xu, J.Y. Pang, Z. Huang, J.J. Wu, Z. Cai, M.D. Yan, C. Sun, Prediction of electrochemical impedance spectroscopy of high-entropy alloys corrosion by using gradient boosting decision tree, Mater. Today Commun. 32 (2022), 104047.
[65] R. Feng, C.A. Zhang, M.C. Gao, Z.R. Pei, F. Zhang, Y. Chen, D. Ma, K. An, J.D. Poplawsky, L.Z. Ouyang, Y. Ren, J.A. Hawk, M. Widom, P.K. Liaw, High-throughput design of high-performance lightweight high-entropy alloys, Nat. Commun. 12 (2021) 1–10.
[66] Y.P. Lu, H.F. Huang, X.Z. Gao, C.L. Ren, J. Gaob, H.Z. Zhang, S.J. Zheng, Q.Q. Jin, Y.H. Zhao, C.Y. Lu, T.M. Wang, T.J. Li, A promising new class of irradiation tolerant materials: Ti2ZrHfV0.5Mo0.2 high-entropy alloy, J. Mater. Sci. Technol. 35 (2019) 369–373.
[67] T.F. Yang, S.Q. Xia, W. Guo, R. Hu, J.D. Poplawsky, G. Sha, Y. Fang, Z.F. Yan, C.X. Wang, C.Y. Li, Y. Zhang, S.J. Zinkle, Y.G. Wang, Effects of temperature on the irradiation responses of Al0.1CoCrFeNi high entropy alloy, Scripta Mater. 144 (2018) 31–35.
[68] T.F. Yang, W. Guo, J.D. Poplawsky, D.Y. Li, L. Wang, Y. Li, W.Y. Hu, M.L. Crespillo, Z.F. Yan, Y. Zhang, Y.G. Wang, S.J. Zinkle, Structural damage and phase stability of Al0.3CoCrFeNi high entropy alloy under high temperature ion irradiation, Acta Mater. 188 (2020) 1–15.
[69] M. Chen, K. Yang, Z. Wang, S. Wang, E. Wu, Y. Lu, Z. Ni, J. Lu, G. Sun, Microstructure evolution and mechanical performance of NV E690 steel repaired by underwater laser directed energy deposition technique, Adv. Powder Mater. (2022), 100095.
[70] L. Zhang, Y. Shibuta, C. Lu, X. Huang, Interaction between nano-voids and migrating grain boundary by molecular dynamics simulation, Acta Mater. 173 (2019) 206–224.
[71] G.R. Odette, N. Almirall, P.B. Wells, T. Yamamoto, Precipitation in reactor pressure vessel steels under ion and neutron irradiation: On the role of segregated network dislocations, Acta Mater. 212 (2021), 116922.
[72] A. Breidi, S.L. Dudarev, Dislocation dynamics simulation of thermal annealing of a dislocation loop microstructure, J. Nucl. Mater. 562 (2022), 153552.
[73] K.Y. Tsai, M.H. Tsai, J.W. Yeh, Sluggish diffusion in Co–Cr–Fe–Mn–Ni high-entropy alloys, Acta Mater. 61 (2013) 4887–4897.
[74] Y.Z. Wang, Y.J. Wang, Disentangling diffusion heterogeneity in high-entropy alloys, Acta Mater. 224 (2022), 117527.
[75] D. Gaertner, J. Kottke, Y. Chumlyakov, F. Hergemoller, G. Wilde, S.V. Divinski, Tracer diffusion in single crystalline CoCrFeNi and CoCrFeMnNi high-entropy alloys: Kinetic hints towards a low-temperature phase instability of the solid-solution? Scripta Mater. 187 (2020) 57–62.
[76] J. Kottke, M. Laurent-Brocq, A. Fareed, D. Gaertner, L. Perriere, L. Rogal, S.V. Divinski, G. Wilde, Tracer diffusion in the Ni-CoCrFeMn system: Transition from a dilute solid solution to a high entropy alloy, Scripta Mater. 159 (2019) 94–98.
[77] G.S. Jawaharram, C.M. Barr, A.M. Monterrosa, K. Hattar, R.S. Averback, S.J. Dillon, Irradiation induced creep in nanocrystalline high entropy alloys, Acta Mater. 182 (2020) 68–76.
[78] J. Dabrowa, W. Kucza, G. Cieslak, T. Kulik, M. Danielewski, J.W. Yeh, Interdiffusion in the FCC-structured Al–Co–Cr–Fe–Ni high entropy alloys: Experimental studies and numerical simulations, J. Alloys Compd. 674 (2016) 455–462.
[79] Y.N. Osetsky, L.K. Beland, A.V. Barashev, Y.W. Zhang, On the existence and origin of sluggish diffusion in chemically disordered concentrated alloys, Curr. Opin. Solid State Mater. Sci. 22 (2018) 65–74.
[80] J. Jiang, Z. Lu, J. Shen, T. Wada, H. Kato, M.W. Chen, Decoupling between calorimetric and dynamical glass transitions in high-entropy metallic glasses, Nat. Commun. 12 (2021) 1–10.
[81] C.M. Barr, E.Y. Chen, J.E. Nathaniel, P. Lu, D.P. Adams, R. Dingreville, B.L. Boyce, K. Hattar, D.L. Medlin, Irradiation-induced grain boundary facet motion: *In situ* observations and atomic-scale mechanisms, Sci. Adv. 8 (2022), eabn0900.
[82] H. Takahashi, N. Hashimoto, Radiation-induced segregation and grain boundary migration in Fe–Cr–Ni model alloy under irradiation, Mater. Trans., JIM 34 (1993) 1027–1030.
[83] N. Li, J. Wang, Y.Q. Wang, Y. Serruys, M. Nastasi, A. Misra, Incoherent twin boundary migration induced by ion irradiation in Cu, J. Appl. Phys. 113 (2013), 023508.
[84] K.Y. Yu, D. Bufford, F. Khatkhatay, H. Wang, M.A. Kirk, X. Zhang, In situ studies of irradiation-induced twin boundary migration in nanotwinned Ag, Scripta Mater. 69 (2013) 385–388.
[85] D.L. Olmsted, S.M. Foiles, E.A. Holm, Grain boundary interface roughening transition and its effect on grain boundary mobility for non-faceting boundaries, Scripta Mater. 57 (2007) 1161–1164.
[86] F.S. Tan, J. Li, H. Feng, Q.H. Fang, C. Jiang, Y. Liu, P.K. Liaw, Entropy-induced transition on grain-boundary migration in multi-principal element alloys, Scripta Mater. 194 (2021), 113668.
[87] L. Koch, F. Granberg, T. Brink, D. Utt, K. Albe, F. Djurabekova, K. Nordlund, Local segregation versus irradiation effects in high-entropy alloys: Steady-state conditions in a driven system, J. Appl. Phys. 122 (2017), 105106.
[88] F. Tuomisto, I. Makkonen, J. Heikinheimo, F. Granberg, F. Djurabekova, K. Nordlund, G. Velisa, H. Bei, H. Xue, W.J. Weber, Y. Zhang, Segregation of Ni at early stages of radiation damage in NiCoFeCr solid solution alloys, Acta Mater. 196 (2020) 44–51.
[89] N.A.P.K. Kumar, C. Li, K.J. Leonard, H. Bei, S.J. Zinkle, Microstructural stability and mechanical behavior of FeNiMnCr high entropy alloy under ion irradiation, Acta Mater. 113 (2016) 230–244.
[90] T. Yang, Y.L. Zhao, W.P. Li, C.Y. Yu, J.H. Luan, D.Y. Lin, L. Fan, Z.B. Jiao, W.H. Liu, X.J. Liu, J.J. Kai, J.C. Huang, C.T. Liu, Ultrahigh-strength and ductile superlattice alloys with nanoscale disordered interfaces, Science 369 (2020) 427–432.
[91] C.M. Barr, J.E. Nathaniel, K.A. Unocic, J.P. Liu, Y. Zhang, Y.Q. Wang, M.L. Taheri, Exploring radiation induced segregation mechanisms at grain boundaries in equiatomic CoCrFeNiMn high entropy alloy under heavy ion irradiation, Scripta Mater. 156 (2018) 80–84.

[92] M. Vaidya, K.G. Pradeep, B.S. Murty, G. Wilde, S.V. Divinski, Bulk tracer diffusion in CoCrFeNi and CoCrFeMnNi high entropy alloys, Acta Mater. 146 (2018) 211–224.
[93] Y. Zhang, W.Q. Jiang, A. Gokhman, J.J. Yang, K. Shi, J.H. Luan, Y. Cui, P.K. Liaw, C.T. Liu, Z.W. Zhang, Enhanced irradiation tolerance of Fe30Cr25Ni20Co15Mn10 high-entropy alloy via nanotwin boundaries, J. Nucl. Mater. 557 (2021), 153292.
[94] T. Nagase, P.D. Rack, J.H. Noh, T. Egami, In-situ TEM observation of structural changes in nano-crystalline CoCrCuFeNi multicomponent high-entropy alloy (HEA) under fast electron irradiation by high voltage electron microscopy (HVEM), Intermetallics 59 (2015) 32–42.
[95] K. Jin, C. Lu, L.M. Wang, J. Qu, W.J. Weber, Y. Zhang, H. Bei, Effects of compositional complexity on the ion-irradiation induced swelling and hardening in Ni-containing equiatomic alloys, Scripta Mater. 119 (2016) 65–70.
[96] G. Pu, L.W. Lin, R. Ang, K. Zhang, B. Liu, B. Liu, T. Peng, S.F. Liu, Q.R. Li, Outstanding radiation tolerance and mechanical behavior in ultra-fine nanocrystalline Al1.5CoCrFeNi high entropy alloy films under He ion irradiation, Appl. Surf. Sci. 516 (2020), 146129.
[97] C. Cabet, E. Dalle, E. Gaganidze, J. Henry, H. Tanigawa, Ferritic-martensitic steels for fission and fusion applications, J. Nucl. Mater. 523 (2019) 510–537.
[98] C.Y. Li, X.X. Hu, T.F. Yang, N.A.P.K. Kumar, B.D. Wirth, S.J. Zinkle, Neutron irradiation response of a Co-free high entropy alloy, J. Nucl. Mater. 527 (2019), 151838.
[99] M. Moorehead, P. Nelaturu, M. Elbakhshwan, C. Parkin, C. Zhang, K. Sridharan, D.J. Thoma, A. Couet, High-throughput ion irradiation of additively manufactured compositionally complex alloys, J. Nucl. Mater. 547 (2021), 152782.
[100] G.S. Was, D. Petti, S. Ukai, S. Zinkle, Materials for future nuclear energy systems, J. Nucl. Mater. 527 (2019), 151837.
[101] M. Moschetti, A. Xu, B. Schuh, A. Hohenwarter, J.P. Couzinie, J.J. Kruzic, D. Bhattacharyya, B. Gludovatz, On the room-temperature mechanical properties of an ion-irradiated TiZrNbHfTa refractory high entropy alloy, JOM 72 (2020) 130–138.
[102] S. Chang, K.K. Tseng, T.Y. Yang, D.S. Chao, J.W. Yeh, J.H. Liang, Irradiation-induced swelling and hardening in HfNbTaTiZr refractory high-entropy alloy, Mater. Lett. 272 (2020), 127832.
[103] C.Y. Lu, T.N. Yang, K. Jin, G. Velisa, P.Y. Xiu, M. Song, Q. Peng, F. Gao, Y.W. Zhang, H.B. Bei, W.J. Weber, L.M. Wang, Enhanced void swelling in NiCoFeCrPd high-entropy alloy by indentation-induced dislocations, Mater. Res. Lett. 6 (2018) 584–591.
[104] T.N. Yang, C.Y. Lu, G. Velisa, K. Jin, P.Y. Xiu, Y.W. Zhang, H.B. Bei, L.M. Wang, Influence of irradiation temperature on void swelling in NiCoFeCrMn and NiCoFeCrPd, Scripta Mater. 158 (2019) 57–61.
[105] M. Schneider, G. Laplanche, Effects of temperature on mechanical properties and deformation mechanisms of the equiatomic CrFeNi medium-entropy alloy, Acta Mater. 204 (2021), 116470.
[106] F.L. Wang, G.H. Balbus, S.Z. Xu, Y.Q. Su, J. Shin, P.F. Rottmann, K.E. Knipling, J.C. Stinville, L.H. Mills, O.N. Senkov, I.J. Beyerlein, T.M. Pollock, D.S. Gianola, Multiplicity of dislocation pathways in a refractory multiprincipal element alloy, Science 370 (2020) 95–101.
[107] M. Naeem, H.Y. He, F. Zhang, H.L. Huang, S. Harjo, T. Kawasaki, B. Wang, S. Lan, Z.D. Wu, F. Wang, Y. Wu, Z.P. Lu, Z.W. Zhang, C.T. Liu, X.L. Wang, Cooperative deformation in high-entropy alloys at ultralow temperatures, Sci. Adv. 6 (2020), eaax4002.
[108] B. Chen, S.Z. Li, H.X. Zong, X.D. Ding, J. Sun, E.A. Ma, Unusual activated processes controlling dislocation motion in body-centered-cubic high-entropy alloys, Proc. Natl. Acad. Sci. U.S.A. 117 (2020) 16199–16206.
[109] T. Zhu, Z.H. Zhong, X.L. Ren, Y.M. Song, F.J. Ye, Q.Q. Wang, A.H.W. Ngan, B.Y. Wang, X.Z. Cao, Q. Xu, Influence of hydrogen behaviors on tensile properties of equiatomic FeCrNiMnCo high-entropy alloy, J. Alloys Compd. 892 (2022), 162260.
[110] X. Yan, P.H. Cao, W.W. Tao, P. Sharma, H.S. Park, Atomistic modeling at experimental strain rates and timescales, J. Phys. D Appl. Phys. 49 (2016), 493002.
[111] S. Curtarolo, G.L.W. Hart, M.B. Nardelli, N. Mingo, S. Sanvito, O. Levy, The high-throughput highway to computational materials design, Nat. Mater. 12 (2013) 191–201.

Fusheng Tan is currently a doctoral researcher at the College of Mechanical and Vehicle Engineering at Hunan University. His research interests are focus on the grain boundaries related deformation and irradiation behaviors of high-entropy alloys using multiscale modelling (*ab initio* calculations and atomic simulations) combined with thermodynamic theories.

Li Li received his Ph.D. degree from Hunan University in 2022. He is currently a postdoctoral researcher at the College of Engineering of Peking University. His current research interests are focused on the design of nickel-based superalloys and high-entropy alloys, using theoretical modelling combined with machine learning.

Jia Li is an associate professor in College of Mechanical and Vehicle Engineering at Hunan University. He received his Ph.D. degree from Hunan University in 2017. His current research interests focus on the deformation and strengthening of high-entropy alloys using multiscale simulation combined with experiment.

Qihong Fang is a professor of Department of Mechanics in Hunan University. He received his Ph.D. degree in 2007 from Hunan University, where he is engaged in the interdisciplinary research of mechanics, mechanical engineering, and material science. His current research interests focus on multiscale mechanics, high-entropy alloys, precision manufacturing, additive manufacturing, high throughput design and preparation of materials, and their service properties.

Bin Liu is a professor of Powder Metallurgy Research Institute in Central South University. He received his Ph.D. degree in 2008 from Central South University. His current research interests focus on the deformation, strengthening, and irradiation behaviors of advanced powder-metallurgy materials.

Peter K. Liaw is a professor and Ivan Racheff Chair of Excellence at the Department of Materials Science and Engineering, The University of Tennessee. He received his Ph.D. degree in 1980 on materials science and engineering from Northwestern University, USA. His current research interests focus on the areas of deformation, fatigue, and fracture of structural alloys and composites, including high-entropy alloys and bulk metallic glasses.